Limnology and Oceanography
FLUIDS & ENVIRONMENTS

ORIGINAL ARTICLE

Hydrodynamics of intertidal oyster reefs: The influence of boundary layer flow processes on sediment and oxygen exchange

Matthew A. Reidenbach,[1] **Peter Berg,**[1] **Andrew Hume,**[1] **Jennifer C. R. Hansen,**[1] **and Elizabeth R. Whitman**[1,2]

Abstract

An intertidal Crassostrea virginica *oyster reef was instrumented to quantify processes affecting boundary layer flow, suspended sediment deposition and erosion, and the flux of oxygen to and from the benthos. Velocity and suspended sediment concentrations were measured at opposing sides of the reef and sediment fluxes, due to the combined effects of deposition, resuspension, and suspension feeding by the reef community, were computed from the difference between upstream and downstream suspended sediment concentrations. At the center of the reef, the flux of oxygen to and from the reef was measured using the eddy-correlation technique. While the reef was submerged, oxygen fluxes showed no significant correlation to light, and oxygen uptake increased linearly with velocity, ranging between 100 and 600 mmol $m^{-2}d^{-1}$. Sediment deposition to the reef also increased linearly for velocities between 0 and 10 cm s^{-1}, up to a maximum of 3500 g $m^{-2}d^{-1}$. For velocities >15 cm s^{-1}, sediment flux to the reef decreased as sediment resuspension occurred due to bed shear stresses that exceeded the critical threshold for erosion. At velocities >25 cm s^{-1}, there was net sediment erosion from the reef. Overall, during summertime and nonstorm conditions, mean oxygen uptake was 270 ± 40 mmol $m^{-2}d^{-1}$ and sediment deposition was 1100 ± 390 g $m^{-2}d^{-1}$ while the reef was submerged, indicating that oysters have a net positive effect on water clarity and that hydrodynamics exert a strong influence on benthic fluxes of oxygen and sediment to and from the reef.*

Keywords: filtration, respiration, turbulence, *Crassostrea virginica*

[1]Department of Environmental Sciences, University of Virginia, Charlottesville, Virginia 22904, USA

[2]Present address: Department of Biological Sciences, Marine Sciences Program, Florida International University, North Miami, Florida 33181, USA

Correspondence to Matthew A. Reidenbach, reidenbach@virginia.edu

Introduction

[1] The suspension-feeding eastern oyster, *Crassostrea virginica* (Gmelin 1791), clears large quantities of organic and inorganic particulate matter from the water column, removing not only phytoplankton but also suspended sediment (Newell 1988; Nelson et al. 2004). In waters subject to anthropogenic and natural nutrient inputs, this tight coupling between the water column and ocean bottom may improve water quality by functioning as an ecologically efficient filter (Lenihan 1999; Zhou et al. 2006). Water clearance rates have been measured for *C. virginica* at >100 L individual^{-1} d^{-1} (Riisgard 1988), and the pseudofeces that are deposited can be one to two times an oyster's dry tissue weight per week (Haven and Morales-Alamo 1966). This substantial biodeposition, which includes the processes of particulate removal, compaction

Limnology and Oceanography: Fluids and Environments • 3 (2013): 225–239 • DOI 10.1215/21573689-2395266

within the animal, and expulsion of feces and pseudofeces (Nelson et al. 2004), can increase particle settling rates up to seven times greater than normal gravity-driven deposition (Dame 1999). Depletion rates of particulates were highest during time periods of enhanced mixing, which are driven by local hydrodynamics, and increase the fraction of the water column available to benthic suspension feeders. This typically occurs during time periods when the ratio of water speed to oyster surface area is greatest (Roegner 1998; Nelson et al. 2004). The three-dimensional benthic structure of the reef, with its substantial roughness, also promotes greater turbulence, which can make more of the particulate matter found within the water column available to suspension feeders (Nelson et al. 2004; Crimaldi et al. 2007; Reidenbach et al. 2007).

[2] Because of suspension feeding by the oyster reef community, input of organic matter from the water column to the benthos influences benthic metabolism (Shumway and Koehn 1982; Dame et al. 1992), and combined with their own metabolic requirements, oysters can make a substantial contribution to total benthic oxygen uptake (Boucher and Boucher-Rodoni 1988). Seasonal fluctuations in oxygen flux over an oyster reef, measured in mesocosms, indicated oxygen uptake that ranged from 22 mmol m^{-2} d^{-1} during the winter to 90 mmol m^{-2} d^{-1} during the summer (Boucher and Boucher-Rodoni 1988). Using in situ portable tunnels that allowed for variations in water flow, Dame et al. (1992) measured annual uptake rates of 6.5 kg m^{-2} (equivalent to 550 mmol m^{-2} d^{-1}) of oxygen along oyster reefs in North Inlet, South Carolina. The sediments found within these shallow aquatic environments typically have high organic matter content due to intense pelagic and benthic primary production, which stimulates oxygen consumption that occurs due to organic matter mineralization and oxidation of reduced compounds (Dedieu et al. 2007). Replenishment of oxygen to the bed is, in part, controlled by both local hydrodynamic processes (Roy et al. 2002; O'Connor and Hondzo 2008) and flow interaction with benthic topography (Dade 1993). Thus, the same shear stress and turbulence processes affecting sediment erosion and deposition also affects oxygen exchange processes at the sediment–water interface. Simultaneous measurements of benthic oxygen uptake and suspended sediment concentrations across the reef would allow the determination of how changes in metabolism of an oyster reef are related to particle removal from the overlying water column and how these processes vary within a natural flow environment.

[3] Measurements of benthic exchange are often accomplished in situ by using sediment cores, chambers, or microelectrodes to quantify mass transport across the sediment–water interface (i.e., Glud et al. 1998; Steinberger and Hondzo 1999; Roy et al. 2002). However, core and chamber measurements block natural water circulation over benthic communities, and the structurally rigid topographic surface of oyster reefs often prohibits measurements using microelectrode profiles (Glud 2008). Over hard surfaces with substantial topography that creates high variability in the thickness and dynamics of the diffusive boundary layer, it is more advantageous to measure the vertical transport of oxygen to and from the bed by using the eddy correlation technique (Berg et al. 2003). In this technique, direct estimates of oxygen flux across the sediment–water interface are made using the cross-correlation of simultaneous measures of oxygen concentration and vertical velocity. The benefit of this approach is that, unlike enclosure methods, it gives a nonintrusive measure of oxygen flux that does not impede the natural flow or behavior of the organisms (Berg et al. 2009).

[4] Within Virginia coastal bays, the shallow depths (typically < 2 m) make the bottom sediments susceptible to current-induced sediment suspension due to bed shear stresses that exceed the critical threshold for erosion (Hansen and Reidenbach 2012). Because of low pelagic primary productivity in the coastal bays, light attenuation is controlled primarily by suspended sediment (McGlathery et al. 2001). Currently, large-scale efforts to increase populations of *C. virginica* are under way within the Chesapeake Bay and coastal bays along the Virginia coast of the United States (Breitburg et al. 2000; Coen and Luckenbach 2000). As a result, increased oyster populations may reduce turbidity, improve water quality (Newell and Koch 2004), and create a positive feedback for growth of seagrass beds currently undergoing restoration within adjacent bays (McGlathery et al. 2012). The goal of this

study is, therefore, to determine how the topography of the oyster reef alters the magnitude of flow and turbulence within the bottom boundary layer, and how these hydrodynamic processes, combined with suspension feeding by the benthic community, affect the flux of oxygen and sediment to and from the reef.

Methods

Study Site

[5] Field studies were performed over an intertidal *C. virginica* oyster reef along the Virginia coastline of the United States. The reef is an approximately 270 m^2 mature oyster bed (14 m wide and 20 m long) and is part of a network of numerous healthy patches of oyster reefs surrounding an oyster restoration area operated by The Nature Conservancy (Whitman and Reidenbach 2012). The reef is located ~1 km off the Eastern Shore of Virginia, within the Virginia Coast Reserve (Fig. 1). The Virginia Coast Reserve is characterized by contiguous marsh, shallow bay, and barrier island systems and is a National Science Foundation Long-Term Ecological Research program site. The reef is along the bank of an ~100-m-wide channel that is ~2–3 m deep, where water currents are tidally driven and create flows in the direction parallel to the main axis of the channel during flood and ebb. The reef elevation is highest at its center and decreases in elevation by ~0.75 m at the reef edge. The reef is located within a protected coastal bay, and no observable wave activity (significant wave heights < 0.1 m) was measured during our sampling time period. A mean density of 490 ± 50 oysters m^{-2} (mean ± SE, $n = 16$ sample sites) was measured for oysters with shell lengths >70 mm, using 25-cm × 25-cm quadrats placed randomly on the reef. Sediment grain size diameter, measured within an adjacent coastal bay, was $D_{84} = 157 \pm 7$ μm (Hansen and Reidenbach 2013), where D_{84} is the sediment grain size diameter for which 84% of the sample grain diameters are smaller.

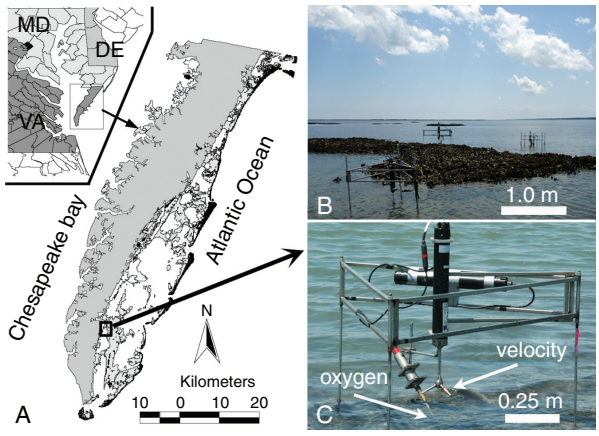

Fig. 1 Experiment location, offshore of Oyster, Virginia, on the southern Delmarva Peninsula, coordinates 37° 16′ 54″ N, 75° 54′ 21″ W (A). Areas shaded gray are land, and offshore regions shaded black along the eastern border are barrier islands. *C. virginica* oyster reef containing velocity and suspended sediment sensors along the edges of the reef and an eddy-correlation system and acoustic Doppler current profiler on the center of the reef (B). Eddy-correlation instrumentation, containing an acoustic Doppler velocimeter and integrated oxygen microsensor that samples oxygen and velocity at 64 Hz within the same water volume (C).

Observational Setup

[6] The *C. virginica* oyster reef was instrumented with sensors to simultaneously measure flow, suspended sediment, and oxygen fluxes. Two acoustic Doppler velocimeters (ADVs; Vector, Nortek, Norway) were deployed 13.5 m apart on opposite ends of the reef and used to measure mean flow at $z = 0.15$ m above the seafloor. The sensors were positioned along an axis parallel to the tidal channel and, because of the alongshore nature of the tidally driven current through the channel, were aligned on the same flow path defined by the dominant direction of flow for both flood and ebb conditions. On each of the two frames holding the ADVs, sediment concentrations were measured with optical backscatter sensors (OBSs; 3+, Campbell Scientific, USA). Both velocities and sediment concentrations were recorded at 64 Hz. To perform laboratory calibrations of the OBSs, sediment samples collected adjacent to the oyster reef were collected, dried, and weighed. Dried sediment was mixed in known quantities into 60-L filtered seawater, and a linear regression was formed between backscatter intensity from the OBS and suspended sediment concentration. Both OBSs were independently calibrated, each having a linear correlation between backscatter intensity and sediment concentration of $R^2 > 0.99$.

[7] At the center of the reef, an ADV was connected via a custom-made amplifier to a Clark-type oxygen microelectrode (Revsbech 1989), and concurrent velocities and oxygen concentrations were measured within the same sampling volume at $z = 0.15$ m above the reef

surface at a sampling rate of 64 Hz. Flow profiles throughout the water column were measured using a high-resolution current profiler (Aquadopp, Nortek) that obtained three-dimensional velocity data in 0.03-m vertical increments between $z = 0.11$ m and 0.86 m above the bed at a sampling rate of 1 Hz. Because of the reef's elevation with respect to the water surface, oysters were submerged for approximately half of the tidal cycle, and water velocities, sediment, and oxygen fluxes were quantified only when all the instruments were submerged. Four deployments, lasting 24 h each, were conducted between 12 June and 24 June 2008.

Sediment Flux Measurements

[8] Sediment flux to and from the oyster reef community was determined by measuring the difference between upstream and downstream suspended sediment concentrations (mg L^{-1}). Deposition of sediment to the reef can occur from active suspension feeding by the bivalve community or by passive physical settlement, whereas sediment erosion can be due to local bed shear stresses driving sediment resuspension combined with mean flow and turbulence that transports sediment away from the reef. Assuming that the water column is well mixed and that the sediment flux is constant across the width of the reef, the sediment flux per unit area of the reef (g m^{-2} d^{-1}) can be computed as

$$\text{sediment flux} = -UH[\text{SSC}_{\text{upstream}} - \text{SSC}_{\text{downstream}}]/L, \quad (1)$$

where U is the depth averaged velocity computed from the velocity profile obtained at the center of the reef, H is the water depth above the reef, $\text{SSC}_{\text{upstream}}$ and $\text{SSC}_{\text{downstream}}$ are the suspended sediment concentrations along the upstream and downstream side of the reef, and L (13.5 m) is the length of reef between the upstream and downstream locations of concentration measurements. Eq. 1 estimates the net sediment flux to the bed and includes all processes involved in sediment deposition and entrainment, including biodeposition of sediment by bivalve feeding activity, passive settlement of particles, and local resuspension. A negative flux indicates net sediment deposition to the seafloor. Mean velocities and sediment fluxes were computed over 15-min averaging intervals. Eq. 1 assumes that SSC values measured at $z = 0.15$ m are representative of average SSC values within the water column and that suspension feeding rates are uniform across the reef. Although measurements at only one location within the water column induce error in the calculation of flux if a vertical concentration gradient exists, because of the extremely shallow nature of the flows a vertically homogeneous SSC assumption was deemed appropriate. Only those flows that were aligned along the axis of the sediment sensors (within ±15°) in the upstream–downstream direction were included in the analysis to minimize errors in sediment flux due to cross-stream flows. This upstream–downstream "control volume" technique was utilized to quantify sediment fluxes rather than through the typical use of sediment traps because we were interested in quantifying both deposition and erosion dynamics across the reef on short time scales, and sediment traps do not provide accurate information about the fluxes of particles in dynamic, high-energy environments (Storlazzi et al. 2011).

Eddy correlation measurement of oxygen fluxes

[9] The vertical oxygen flux within the water column due to advection and molecular diffusion is (Berg et al. 2003)

$$\text{oxygen flux} = wc - D\frac{\partial c}{\partial z}, \quad (2)$$

where w is the instantaneous vertical velocity, c is the oxygen concentration, D is the molecular diffusivity of oxygen in water, and z is the vertical coordinate. Typically, instantaneous values of velocity and concentration are separated into their respective time-averaged ($\bar{w}$) and turbulent (w') fluctuations as $w = \bar{w} + w'$ and $c = \bar{c} + c'$. These separations are then substituted into Eq. 2 and averaged over a time period significantly longer than the time scale of turbulent fluctuations. In addition, when oxygen and velocity measurements are made outside of the diffusive boundary layer adjacent to the sediment–water interface, which is typically less than a millimeter thick, turbulent transport dominates,

and the diffusive component ($-D\partial c/\partial z$) in Eq. 2 can be ignored (Berg et al. 2003; Boudreau and Jorgensen 2001). This simplifies the time-averaged oxygen flux to

$$\overline{\text{oxygen flux}} = \overline{w'c'}. \quad (3)$$

[10] The oxygen flux was computed by averaging over 15-min sampling intervals. This time period was chosen because in statistical examinations of turbulence and oxygen fluxes, 15 min emerged as giving an acceptable balance between including major turbulent fluctuations adding to the flux and minimizing drift in the means of velocity and oxygen due to changes in tidal flow and oxygen exchange processes (Berg et al. 2003). From the three-dimensional velocity measurements (u, v, and w), which were all measured at $z = 0.15$ m above the oyster reef, a coordinate system in which the x-direction is aligned with the mean flow direction was utilized. In practice, it is impossible to position the ADVs so that its coordinates match this system exactly. Therefore, a two-step coordinate rotation was performed for each 15-min time interval so that $\bar{v} = \bar{w} = 0$. The first rotation around the z-axis was performed to nullify the y-component of the mean velocity ($\bar{v} = 0$), and the second rotation around the y-axis was performed to nullify the vertical mean velocity ($\bar{w} = 0$). While the z-axis rotation ranged anywhere between $\pm 180°$ because of the change in tidally dominated flow direction, the y-axis rotation was typically $< \pm 8°$. For each burst, fluctuating components of the vertical velocity and oxygen concentration were then computed by subtracting the means, computed as least-squares linear fits to the measured vertical velocity and oxygen concentration.

Results

Flow Structure and Bed Shear Stress

[11] Depth-averaged mean currents above the reef ranged from 0 to 30 cm s^{-1} and changed direction depending on ebb or flood conditions within the tidal channel. For a well-developed turbulent boundary layer, an inertial sublayer region exists where mean velocities exhibit a logarithmic profile. Within this region, the mean velocity profile is related to the generation of turbulence by shear at the bed, and the "law of the wall" takes the form (Schlichting and Gersten 2000)

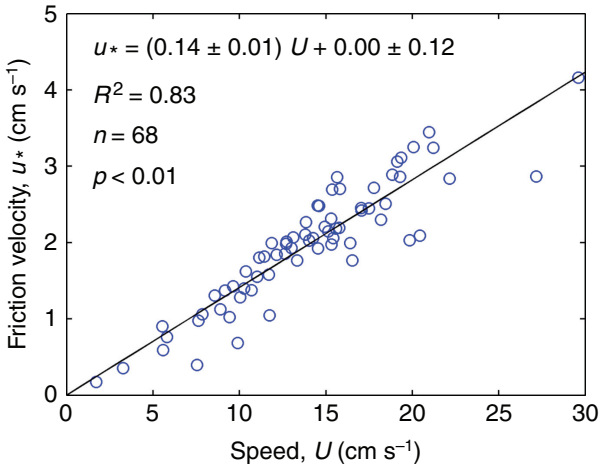

Fig. 2 Friction velocity, u_*, as a function of mean water speed across the oyster reef.

$$U(z) = \frac{u_*}{\kappa}\ln\left(\frac{z-d}{z_o}\right), \quad (4)$$

where $\kappa = 0.41$ is von Karman's constant, u_* is the friction velocity, z is the height above the bed, z_o is the roughness height, and d is the zero plane displacement (Stacey et al. 1999). The friction velocity is defined by $\tau_{bed} = \rho u_*^2$ (Schlichting and Gersten 2000), where τ_{bed} is the bed shear stress and $\rho = 1023$ kg m^{-3} is the density of water. For the oyster reef, the zero plane displacement was estimated to be $d = 5$ cm, which was set equal to the mean elevation of the oysters above datum, and accounts for elevation changes due to the vertical orientation of the oysters. Values of u_* and z_o were adjusted to obtain a best fit through the logarithm of the mean velocity profile. Fourteen measurement points from the current profiler positioned at the center of the reef were used in the fit, at locations between $z = 0.11$ m and 0.50 m above bottom. Below $z = 0.11$ m, flow data were not collected owing to the minimum sampling distance of the instrument, whereas above $z = 0.50$ m a deviation from a logarithmic profile occurred, likely due to wind stress at the surface. To ensure a well-defined log region over the measurement points used in the fit, only profiles having an $R^2 > 0.95$ fit in the log domain were used

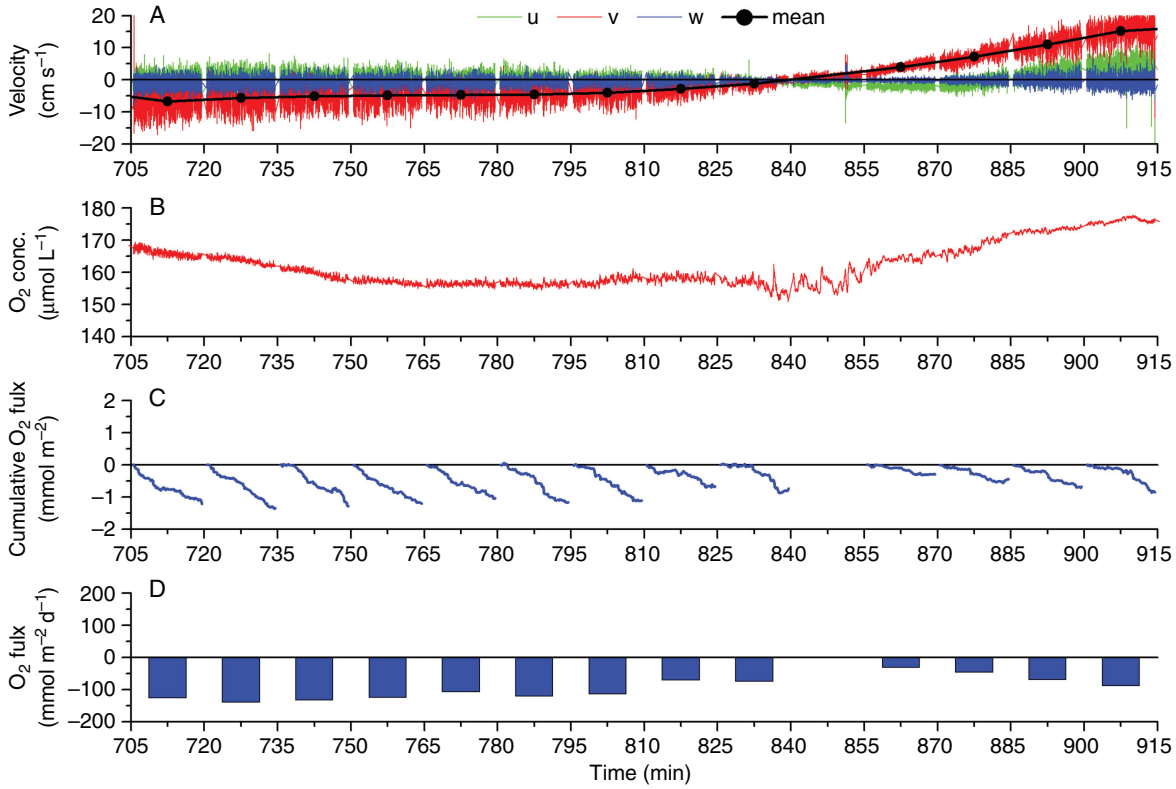

Fig. 3 Time record of water velocity (A), oxygen concentration (B), cumulative oxygen flux (C), and total oxygen flux measured over the oyster reef (D) for each 15-min sampling burst. Negative flux values represent an uptake by the reef. Time = 0 min is the start of the deployment. The time period covers from 02:15 to 05:45 EST on 13 June 2008.

in the analysis. A median value of $z_o = 2.7$ cm was measured. As the velocity of the mean flow increases, $u_\star$ increased linearly from $u_\star = 0$ cm s^{-1} at slack tide to a maximum value of 4.1 cm s^{-1} during peak ebbing flows, with median $u_\star = 1.6$ cm s^{-1} (Fig. 2). Using estimates of the friction velocity, τ_{bed} increased with mean velocity across the reef, from $\tau_{bed} = 0$ Pa at slack tide to a maximum value of $\tau_{bed} = 1.8$ Pa.

[12] The drag coefficient (C_D) was computed using the equation (Schlichting and Gersten 2000)

$$C_D = \frac{u_\star^2}{U_o^2}, \quad (5)$$

where U_o is the current speed at $z = 0.5$ m. The mean drag coefficient for the reef was $C_D = 0.019 \pm 0.004$, which is approximately six times larger than the value of $C_D = 0.003$ typically reported for flows over sands or muds (Gross and Nowell 1983). The drag coefficient can also be estimated from Reynolds stress measurements, computed from velocity fluctuations collected from the same instrument used to measure the flux of oxygen, as $u_\star^2 = -\overline{u'w'}$ (Rippeth et al. 2002). Utilizing Reynolds stress values, $C_D = 0.021 \pm 0.004$, which shows close agreement to the drag coefficient estimated from logarithmic fits to the mean velocity profile.

Oxygen Uptake by the Oyster Reef Community

[13] Water velocities, oxygen concentrations, and cumulative and total oxygen fluxes over a 4-h period, including both flooding and ebbing periods of the tide, are shown in Fig. 3. The record was obtained during nighttime conditions to minimize oxygen production due to photosynthesis by benthic algae. A 4-h period constitutes the entire time period over which measurements could be obtained per tidal cycle because the instrumentation requires water depths of ≥0.3 m over the reef. Oxygen concentrations ranged from 150 to 180 µmol L^{-1} and tended to increase with water speed.

Large fluctuations in oxygen occurred for a 30-min period surrounding high tide, where velocities near 0 cm s^{-1} minimized turbulent mixing (corresponding to time periods between $t = 830$ and 860 min in Fig. 3B). Cumulative oxygen fluxes (Fig. 3C) during each 15-min burst sampling period were calculated by integrating instantaneous estimates of $w'c'$ over time. Smooth linear trending values of the cumulative oxygen flux indicate steady fluxes over the 15-min period, and variability in the linearly trending cumulative record (as seen during slack tide, time = 850 min) indicates changes in the flux or a poorly defined flux signal due to weak turbulent mixing. Negative fluxes indicate uptake of oxygen by the reef community, whereas positive oxygen fluxes indicate release of oxygen. The total flux (Fig. 3D) is the value of the cumulative oxygen flux at the end of the 15-min period, converted to a daily flux of mmol m^{-2} d^{-1}. Fluxes, based on these 15-min periods, ranged from −40 to −140 mmol m^{-2} d^{-1} for the 4-h measurement period shown, whereas maximum uptake rates over the total 4-d record reached −600 mmol m^{-2} d^{-1}. Plotted as a function of mean current speed above the reef, uptake of oxygen by the reef community increased linearly with increasing currents, with $R^2 = 0.75$ (Fig. 4). There was no statistical difference between oxygen fluxes measured during ebb or flood tidal conditions in response to changes in mean current. In addition, oxygen fluxes did not show any statistically significant correlation to ambient light intensity, indicating that measured fluxes represent an uptake by the reef community and were not appreciably altered through photosynthesis by benthic algae.

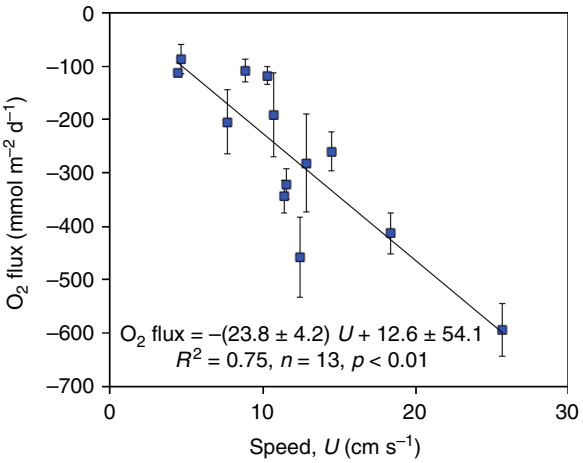

Fig. 4 Total oxygen flux (mean ± SE) as a function of mean water speed, measured at $z = 0.15$ m at the center of the reef. Fluxes that were included consist of nighttime periods when the oxygen and velocity sensors were fully submerged, and the cumulative flux signal (Fig. 3C) showed a clear linear trend. Fluxes were computed as the average of multiple, continuous 15-min bursts and are plotted relative to their corresponding mean U. Only the standard error in the flux is shown, with n ranging from 4 to 13.

Frequency Analysis

[14] The spectrum of the vertical velocity, S_{ww} (Fig. 5A), shows a distinct −5/3 slope, indicative of a well-defined inertial subrange. The flattening of the spectra at high frequencies, at approximately $f > 20$ Hz, indicates that a noise floor in the velocity measurements has been reached and corresponds to $S_{ww} = 10^{-2}$ cm^2 s^{-2} Hz^{-1}. Spectra for c' (Fig. 5B) also show a distinct −5/3 slope within the inertial subrange. The noise floor for oxygen measurements is estimated at the frequency where the spectrum flattens and remains relatively constant, which occurs at $S_{O_2} \sim 10^{-3}$ μmol^2 L^{-2} Hz^{-1}. The oxygen electrode's response time is $t_{90\%} \leq 0.3$ s, and therefore the sensor cannot resolve oxygen fluctuations much faster than ~3 Hz. For $f > 3$ Hz there is an expected drop-off in the spectrum, down to the noise level. Using Taylor's frozen turbulence hypothesis where advection of turbulence past a fixed point can be assumed to be entirely due to the mean flow, frequency was converted to wavenumber as $k = f/U$ (MacMahan et al. 2012) and is shown on the upper x-axis in Fig. 5. The contribution of the flux at different eddy frequencies can be computed through the cumulative cospectrum between w' and c' (Fig. 5C). The spectra is formed over a 15-min record and indicates that the dominant contribution to the flux occurs in frequencies between $f = 0.02$ Hz (or 50 s) and 1 Hz (or 1 s). There is little contribution to the flux at frequencies faster or slower than this, indicating that all relevant scales of motion that contribute to the flux are included in the measured data record.

Oyster Surface Area That Contributes to the Flux

[15] The size and shape of the surface area, the so-called footprint, that contributes to the oxygen flux can be estimated from empirical correlations derived by Berg et al. (2007). The friction velocity (u_*) exerts a major

control on the rate of turbulent mixing in the water column, which is typically quantified as a turbulent eddy diffusivity (K). The vertical eddy diffusivity, K_z, was estimated as $K_z = \kappa u_* z$. Isotropic turbulence was assumed, such that $K_z = K_y = K_x$. From this, the three-dimensional mathematical formulation for solute transport in a turbulent flow was solved analytically to determine the downstream transport and dispersion of a dissolved conservative tracer:

$$\frac{\partial \bar{C}}{\partial t} = \frac{\partial}{\partial x}\left((D+K_x)\frac{\partial \bar{C}}{\partial x}\right) + \frac{\partial}{\partial y}\left((D+K_y)\frac{\partial \bar{C}}{\partial y}\right) + \frac{\partial}{\partial z}\left((D+K_z)\frac{\partial \bar{C}}{\partial z}\right) - \bar{u}\frac{\partial \bar{C}}{\partial x} \quad (6)$$

Eq. 6 contains only an advective term in the direction of the mean current velocity (x-direction). The size and shape of the footprint that contributes to the flux for the measuring height above the reef ($z = 0.15$ m), and various water depths (H), friction velocities (u_*), roughness heights (z_o) were determined. A rougher benthic surface results in more vigorous turbulent mixing that transports the flux signal faster upward toward the measuring point and reduces the length of the footprint. For the oyster reef studied, the measurement location was at the center of the reef, with dense oyster cover extending a distance of 7 m in either direction along the dominant direction of flow. A first-order estimation of the footprint, following the procedure of Berg et al. (2007), indicates that the oyster reef contributed 70%–90% of the measured oxygen flux. From this analysis, the upstream distance from the measuring point to the location with the largest flux contribution can also be estimated as $x_{max} = 1.7$ m. This indicates that although the reef is not large, because of vigorous mixing these flux measurements accurately represent processes occurring on the reef and are not due to benthic activity from surfaces located farther upstream.

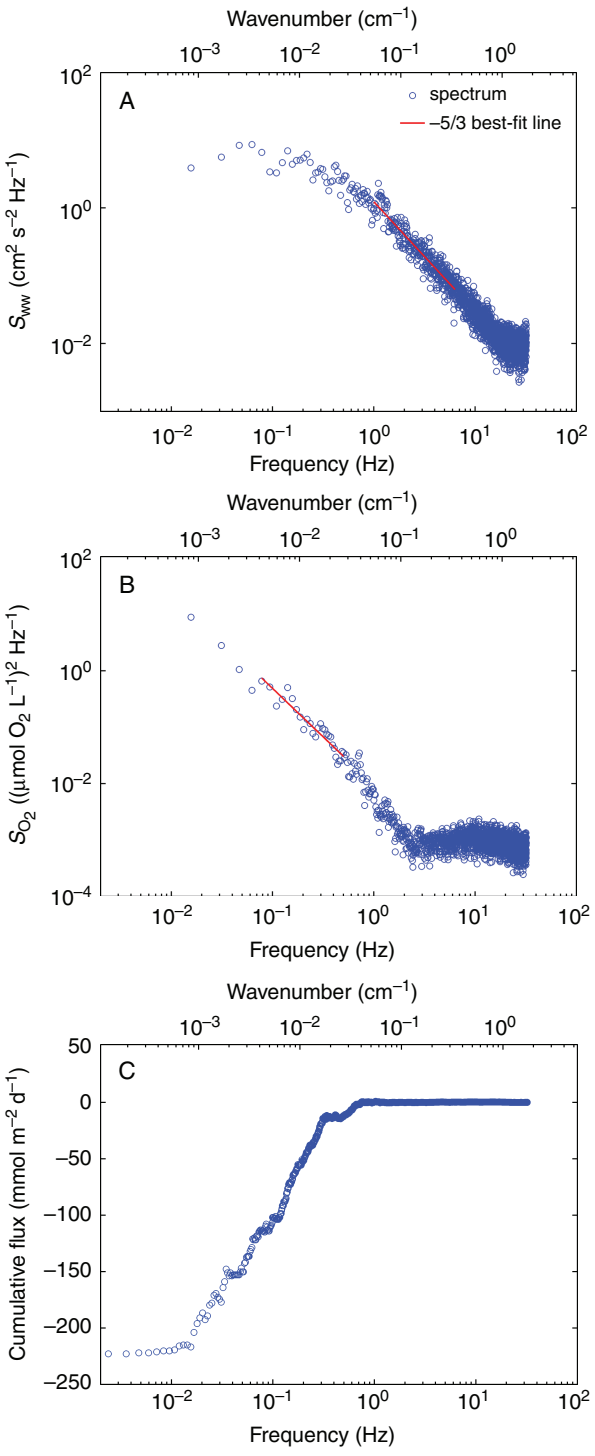

Fig. 5 Spectrum (S_{ww}) for the vertical velocity fluctuations measured using an ADV at a sampling rate of 64 Hz, located $z = 15$ m above the oyster reef (A). Thirteen separate $n = 4096$ vertical velocity subsamples were averaged, corresponding to a 15-min sampling window with $U = 18.5$ cm s^{-1}, to generate the spectrum. Note agreement to predicted −5/3 power law of dissipation of turbulent energy within the inertial subrange. Spectrum (S_{O_2}) for oxygen fluctuations measured using an oxygen microelectrode, showing a −5/3 slope region (B). Both velocity and oxygen spectra are from the same 15-min sampling record. Cumulative oxygen flux as a function of sampling frequency, indicating that the dominant contribution to the flux occurs on time scales between 50 s (or 0.02 Hz) and 1 s (or 1 Hz) (C). The cumulative oxygen flux was not separated into 13 separate subsamples to preserve the full range of frequencies measured.

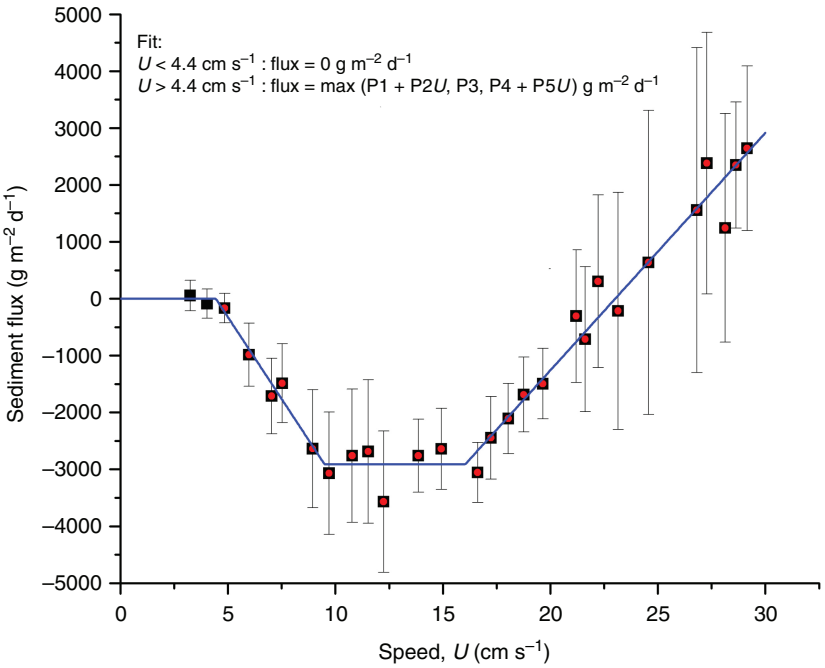

Fig. 6 Net sediment flux measured across the reef as a function of mean horizontal water speed. Negative values indicate deposition and positive values indicate erosion of sediment from the reef. Error bars indicate ±1 SD of the mean flux estimate computed as a running mean over an averaging window of ±2.5 cm s^{-1}. Values for coefficients are P1 = 2550 ± 500 (n = 5), P2 = −580 ± 70 (n = 5), P3 = −2910 ± 1070 (n = 6), P4 = −9610 ± 570 (n = 15), and P5 = 420 ± 20 (n = 15), with cumulative $R^2 = 0.96$ and $p < 0.01$ for linear fits across entire data set. Coefficients were computed independently as the linear best-fit across each velocity range of 4.4 – 9.5 cm/s for P1, P2; 9.5 – 16 cm/s for P3; and 16 – 30 cm/s for P4, P5.

[16] Uncertainty in the footprint estimation and contribution to the flux is due primarily to changes in reef slope and varying water depth (Berg et al. 2007). In addition, accelerations and decelerations in the flow due to its changing tidal conditions or seafloor elevation can also significantly alter the near bottom current profile, leading to inconsistencies in estimates of both u_* and z_o (Lorke et al. 2002). These inconsistencies arise because there is a phase lag between the development of the logarithmic layer of the mean flow and the development of turbulence within the boundary layer. In general, u_* estimates in which the log-profile method is used tend to overestimate values by 5%–25% compared with u_* values computed using Reynolds stress estimates within the boundary layer, that is, $u_*^2 = |\overline{u'w'}|$ (Rippeth et al. 2002). Lu et al. (2000) suggests that discrepancies may be due to horizontal inhomogeneity caused by bedforms, and changes in bed roughness or elevation can significantly distort the mean flow and turbulent structure of boundary layer. However, good agreement was found when computing C_D from u_* estimates computed both from a logarithmic fit to the mean velocity profile and from Reynolds stress, suggesting that the boundary layer may have come to equilibrium when reaching the center of the reef.

[17] Antonia and Luxton (1971) found that the vertical growth of a boundary layer due to a change in bed roughness occurs at ~1/20th the horizontal downstream distance. Velocity measurements were obtained ~7 m from the edge of the reef in either ebb or flood flow directions; therefore, the boundary layer was ~z = 0.35 m thick at the location of measurements. This suggests that oxygen flux measurements obtained at z = 0.15 m were well within the boundary layer formed by the oyster reef, but u_* and z_o estimates from log-profiles obtained between z = 0.11 m and 0.50 m may have been affected by upstream variations in bed roughness and elevation, which altered form drag in the outer boundary layer. Whitman and Reidenbach (2012) conducted a study of flows along mudflats and found that u_* was reduced by a factor of 2 and z_o was reduced by a factor of 5 compared with flows over an adjacent oyster reef. This would suggest that u_* and z_o estimates over the oyster reef might be slightly underpredicted because of contributions to the outer boundary layer from upstream flows over mudflats. Although increases in u_* and z_o would tend to reduce the overall size of the footprint and increase the contribution of the flux originating from the reef, ultimately it is difficult to determine how these topographic variations would alter oxygen flux measurements from the reef without a detailed study of upstream topography.

Sediment Deposition/Erosion by the Benthic Community

[18] Suspended sediment concentrations along the edges of the oyster reef ranged from 25 mg L^{-1} to

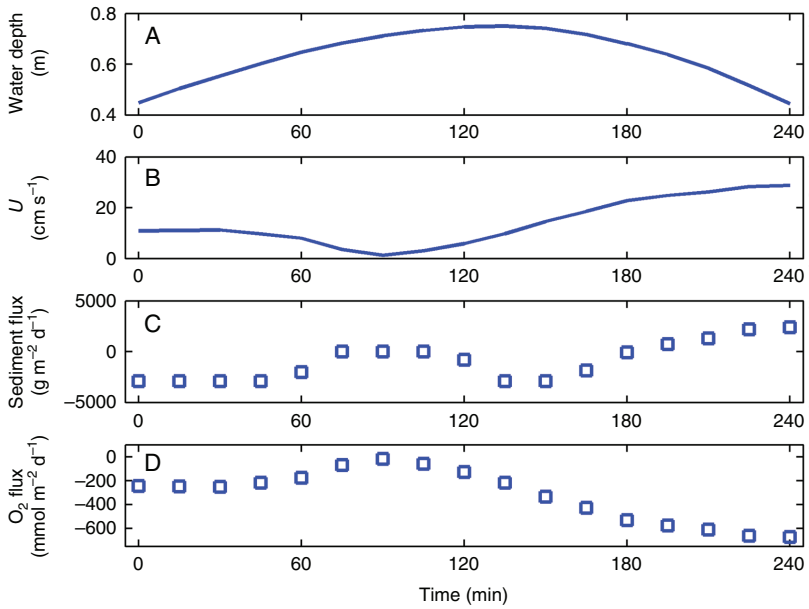

Fig. 7 Measured water depth (A) and water speed (B) over the oyster reef during a tidal cycle, along with estimated sediment flux (C) and oxygen flux (D) from least squares regression fits to the observed flux measurements (as shown in Figs. 4 and 6).

105 mg L^{-1}, with a mean concentration of 55 mg L^{-1}. Net vertical fluxes of sediment to or from the reef community as a function of mean current speed are shown in Fig. 6. For flows below ~25 cm s^{-1}, fluxes were negative, indicating deposition of sediment to the reef. Above 25 cm s^{-1}, fluxes were positive, indicating sediment suspension and transport away from the reef. The maximum deposition rate was -3500 ± 1200 g m^{-2} d^{-1}, which occurred at a mean flow rate of 10–15 cm s^{-1}, while the peak erosion rate was 2700 ± 1400 g m^{-2} d^{-1}, which occurred at maximum flow rates of ~30 cm s^{-1}. At low current speeds (5–10 cm s^{-1}), the general trend of increased uptake of sediment with flow suggests a positive feedback between suspension feeding and velocity. At intermediate current speeds (10–15 cm s^{-1}), maximum uptake rates were reached. Above these speeds (15–30 cm s^{-1}), the rate of sediment deposition decreased, because of the initiation of sediment suspension from the bed. Linear fits to these three separate flow ranges had a coefficient of determination of $R^2 = 0.96$. Averaged over all flow conditions during the 4-d sampling period, mean flux was -1100 ± 390 ($n = 124$) g m^{-2} d^{-1} when the reef was submerged. However, since the intertidal reef is submerged for only approximately half the day (the total time period submerged each day changes with variations in tidal magnitude), sediment flux to the reef integrated over a 24-h period is approximately -550 g m^{-2} d^{-1}, indicating that the oyster reef creates a net reduction of suspended sediment within the overlying water column.

[19] Using best-fit correlations between current speed and oxygen and sediment fluxes, as shown in Figs. 4 and 6, respectively, a 4-h record of measured water depths and velocities surrounding high tide was used to quantify sediment and oxygen flux across the oyster reef (Fig. 7). Estimated sediment flux was near zero during slack water conditions (Fig. 7C); sediment deposition to the reef was highest during rising tide conditions when water currents were 10–15 cm s^{-1}, and sediment erosion occurred during falling tide when mean water currents were >25 cm s^{-1}. The estimated oxygen flux (Fig. 7D) was always negative and was greatest during falling tide (ebb) conditions, when water velocities were greatest.

Discussion

Oxygen Uptake by the Reef Community

[20] The use of the eddy-correlation technique provides an integrated measure of oxygen flux over the reef, which includes not only metabolism by the oysters but also exchanges due to microbial activity within the sediment, metabolism by other cryptic organisms living on the reef, and photosynthesis by plants and algae. The latter was found not to be a significant fraction of the flux since day–night variations in oxygen uptake rates were not statistically different. In addition, within an adjacent shallow coastal bay, daily averages of oxygen flux over bare sediment were -35.4 ± 13.5 mmol m^{-2} d^{-1} when using the same technique (Hume et al. 2011). This suggests that respiration by microbial activity within oyster reef sediments may constitute some fraction of the net uptake, but the majority of the flux is likely due to activity by the oysters

themselves. Oxygen uptake, which ranged from −100 to −600 mmol m^{-2} d^{-1}, represents very high respiration rates by the reef community that were enhanced significantly by water flow (Fig. 4). These are substantially higher uptake rates than found in chamber measurements of oxygen flux measured over oyster reefs, where typical summertime values are approximately −100 mmol m^{-2} d^{-1} (Boucher and Boucher-Rodoni 1988). However, this level of flux corresponds well to our observed fluxes measured during periods of low flow ($U < 5$ cm s^{-1}; Fig. 4), indicating the inherent biases encountered when using chambers that exclude natural flows. Similar discrepancies were found by Berg and Huettel (2008) and P. Berg (University of Virginia, unpubl.) in parallel eddy correlation and chambers measurements over permeable sediments. In comparison, a 10-m-long flume placed in situ over an oyster reef, which allowed free movement of the flowing water, was used by Dame et al. (1992) to quantify the net annual oxygen uptake for an oyster reef. By measuring the upstream–downstream difference in oxygen concentration, an annual uptake of 6.5 kg m^{-2} of oxygen was found, which corresponds to a daily average of −550 mmol m^{-2} d^{-1}, similar to peak measurements we obtained by eddy-correlation but roughly double our daily averaged estimate of −270 ± 40 mmol m^{-2} d^{-1}.

Suspended Sediment Dynamics

[21] Sediment fluxes to the benthos were positively correlated with mean flows for velocities < 10 cm s^{-1}, indicating that either the rate of pumping by oysters increased (the volume of water passing through the siphon per unit time) or enhanced turbulent mixing reduced the thickness of concentration boundary layers near the reef surface and allowed for more of the water column to be available to them (O'Riordan et al. 1993). Sediment fluxes to the reef peaked at 10–15 cm s^{-1} and were reduced at greater velocities, suggesting that at velocities >10–15 cm s^{-1} a critical stress threshold had been reached to initiate sediment erosion. This corresponds to a bed shear stress of $\tau_{bed} = 0.2–0.4$ N m^{-2}. These values agree closely with results obtained by Dame et al. (1985), who found that most uptake of particles over *C. virginica* reefs in North Inlet, South Carolina, took place at water velocities < 15 cm s^{-1}, whereas resuspension of sediment occurred at velocities > 15 cm s^{-1}. At our site, above ~25 cm s^{-1}, net sediment flux was positive, indicating resuspension rates that were greater than the combined rates of suspension feeding and particle deposition, producing conditions of net transport of sediment from the reef. Flume studies by Widdows et al. (1998) found deposition rates due to mussel beds to be as high as 1440 g m^{-2} d^{-1}, and at greatest measured mussel densities the presence of bivalves reduced sediment erosion by 10-fold. However, a shift from biodeposition to erosion occurred at a critical threshold of 20–25 cm s^{-1}, similar to our in situ measurements for the oyster reef.

[22] The average benthic deposition rate for sediment, α, can be computed as

$$\alpha = -\frac{\overline{\text{flux}_{ssc}}}{\overline{SSC}}, \tag{7}$$

where $\overline{SSC}$ (g m^{-3}) is the mean suspended sediment concentration, $\overline{\text{flux}_{ssc}}$ (g m^{-2} d^{-1}) is the mean sediment flux, and α (m d^{-1}) is a measure of net removal of sediment by the reef community. Over the oyster reef, the mean sediment $\overline{\text{flux}_{ssc}} = -1100$ g m^{-2} d^{-1} when the reef was submerged, while average suspended sediment concentration in the water column during the same time period was $\overline{SSC} = 48$ g m^{-3}. This is equivalent to a benthic clearance rate of $\alpha = 23.5$ m d^{-1}. This indicates that when submerged, the reef would clear suspended sediment from a water volume equivalent to an ~23.5-m-deep column of water above the reef in 1 d. Since the intertidal oyster reef is only submerged for approximately half of the day, daily clearance rates for sediment would be half these values. Average sediment flux over farmed Pacific oysters (*Crassostrea gigas*) in Australia during a 3-d period in the summer was found to be −180.5 g m^{-2} d^{-1} (Mitchell 2006), substantially lower than rates found over the *C. virginica* reef studied here. However, $\overline{SSC} = 12.1 \pm 8.7$ g m^{-3} was also substantially lower, giving $\alpha = 14.9$ m d^{-1}. In addition, *C. gigas* densities were measured at 360 oysters m^{-2} on oyster racks, compared with the *C. virginica* reef density of 490 ± 50 oysters m^{-2}.

[23] The mean sediment deposition rate of 23.5 m d^{-1} is similar to uptake rates of phytoplankton by subtidal coral reefs in the Red Sea at $\alpha = 20 \pm 8$ m d^{-1}

(Genin et al. 2009) but less than within subtidal sponge-dominated reefs of the Florida Keys at $\alpha = 48 \pm 20\ \mathrm{m\ d^{-1}}$ (Monismith et al. 2010). Within San Francisco Bay, phytoplankton uptake rates ranged from $\alpha = 6$ to $50\ \mathrm{m\ d^{-1}}$ for dense patches of bivalve suspension feeders composed primarily of clams (Jones et al. 2009). For all these cases, enhanced suspension feeding on phytoplankton was found under greater mean flow (between $U = 0$ and $50\ \mathrm{cm\ s^{-1}}$) and bed shear-stress conditions (between $u_\star = 0$ and $1.8\ \mathrm{cm\ s^{-1}}$). Laboratory and flow-through chamber experiments by Ackerman and Nishizaki (2004) found either relatively constant or increasing clearance rates of seston with velocity for two species of marine mussels, *Mytilus trossulus* and *M. californianus*. Numerical studies of suspension feeding by intertidal mussel beds (Fréchette et al. 1989) have shown that particle feeding is enhanced by flow-enhanced vertical turbulent transport and a higher rate of replenishment of phytoplankton to food-impoverished near-bottom waters. In both field and numerical studies, no reduction in phytoplankton uptake occurred at highest flow rates, suggesting that bivalves, sponges, and other suspension feeders continue to clear water at high ambient velocities and that resuspension of benthic plankton from the benthos is not a significant contributor to water column plankton levels. This lack of resuspension at high flow rates is not the case for muddy sediment, however; suspended sediment concentrations can be locally enhanced within the Virginia coastal bays due to resuspension from the seafloor (Lawson et al. 2007). Therefore, measurements of α for sediment include co-occurring processes of active suspension feeding, natural deposition, and hydrodynamic-controlled erosion from the reef.

[24] While submerged, mean sediment flux to the reef was $-1100 \pm 390\ \mathrm{g\ m^{-2}\ d^{-1}}$. Assuming that the oyster reef is submerged for half the tidal cycle and that there is a bulk sediment density of $\rho_s = 2.0\ \mathrm{g\ cm^{-3}}$, this is equivalent to an accumulation rate of $\sim 10\ \mathrm{cm\ yr^{-1}}$ of sediment on the reef. However, measurements were conducted during the summer, when suspension feeding is expected to be greater than cold-water winter conditions (Mitchell 2006). Particle removal by *C. virginica* has been shown to increase up to seven times with increasing water temperatures (Newell and Koch 2004). In addition, storm activity, which may periodically generate waves and enhance flow rates to $>25\ \mathrm{cm\ s^{-1}}$ and thus cause sediment erosion from the reef, may exert substantial control on bulk sediment accumulation rates. No storm activity was noted during our experiments, and therefore our measurements of sediment deposition are likely representative of near-peak values during summertime conditions.

[25] Combined, these measurements suggest that oyster metabolism increases linearly with flow, and even though enhanced suspended sediment concentrations occur within the water column under high-flow conditions, this is not due to reductions in the rate of suspension feeding by oysters themselves. Rather, increases in suspended sediment concentrations are due to increased erosion from the reef once critical stress thresholds for sediment suspension are surpassed, which suggests that oysters have a net positive impact on water clarity under all flow conditions.

Significance to Aquatic Environments

[26] Our results show that oysters have a significant positive effect on the deposition of suspended sediment in shallow coastal environments, thereby decreasing turbidity and enhancing light penetration through the water column. This positive effect on water clarity can increase productivity of benthic primary producers. Even though metabolic uptake of oxygen increases linearly with mean current speed, sedimentation rates are variable, and sediment deposition to the reef increases to $3500\ \mathrm{g\ m^{-2}\ d^{-1}}$ at ambient velocities between 10 and $15\ \mathrm{cm\ s^{-1}}$ but decreases at higher flow rates as sediment resuspension from the reef occurs due to enhanced shear stress. Ambient velocities across the reef enhanced oxygen uptake rates up to six times compared with time periods when velocities were near zero. Our results, based on in situ oxygen and sediment measurements, indicate that natural variability in the flow as it interacts with benthic topography is important and that flumes, chambers, and other enclosure approaches must be interpreted with caution when exchange rates for the natural environment are needed.

Acknowledgments We gratefully acknowledge Barry Truitt, Bowdoin Lusk, and The Nature Conservancy for access to oyster sites and

logistical support. A. Schwarzschild, C. Buck, and D. Boyd provided field assistance. This research was funded through Virginia Coast Reserve Long-Term Ecological Research grants by the National Science Foundation (NSF-DEB 0621014 and NSF-DEB 1237733).

References

Ackerman, J. D., and M. T. Nishizaki. 2004. The effect of velocity on the suspension feeding and growth of the marine mussels *Mytilus trossulus* and *M. californianus*: Implications for niche separation. J. Mar. Syst. **49**: 195–207. doi:10.1016/j.jmarsys.2003.06.004.

Antonia, R. A., and R. E. Luxton. 1971. The response of a turbulent boundary layer to a step change in surface roughness: Part 1. Smooth to rough. J. Fluid Mech. **48**: 721–761. doi:10.1017/S0022112071001824.

Berg, P., R. N. Glud, A. Hume, H. Stahl, K. Oguri, V. Meyer, and H. Kitazato. 2009. Eddy correlation measurements of oxygen uptake in deep ocean sediments. Limnol. Oceanogr. Methods. **7**: 576–584. doi:10.4319/lom.2009.7.576.

Berg, P., and M. Huettel. 2008. Monitoring the seafloor using the noninvasive eddy correlation technique: Integrated benthic exchange dynamics. Oceanography **21**: 164–167. doi:10.5670/oceanog.2008.13.

Berg, P., H. Roy, F. Janssen, V. Meyer, B. B. Jorgensen, M. Huettel, and D. De Beer. 2003. Oxygen uptake by aquatic sediments measured with a novel non-invasive eddy-correlation technique. Mar. Ecol. Prog. Ser. **261**: 75–83. doi:10.3354/meps261075.

Berg, P., H. Roy, and P. L. Wiberg. 2007. Eddy correlation flux measurements: The sediment surface area that contributes to the flux. Limnol. Oceanogr. **52**: 1672–1684. doi:10.4319/lo.2007.52.4.1672.

Boucher, G., and R. Boucher-Rodoni. 1988. In situ measurements of respiratory metabolism and nitrogen fluxes at the interface of oyster beds. Mar. Ecol. Prog. Ser. **44**: 229–238. doi:10.3354/meps044229.

Boudreau, B. P., and B. B. Jorgensen [eds]. 2001. The Benthic Boundary Layer: Transport Processes and Biogeochemistry. Oxford University Press.

Breitburg, D. L., L. D. Coen, M. W. Luckenbach, R. Mann, M. Posey, and J. A. Wesson. 2000. Oyster reef restoration: Convergence of harvest and conservation strategies. J. Shellfish Res. **19**: 371–377.

Coen, L. D., and M. W. Luckenbach. 2000. Developing success criteria and goals for evaluating oyster reef restoration: Ecological function or resource exploitation? Ecol. Eng. **15**: 323–343. doi:10.1016/S0925-8574(00)00084-7.

Crimaldi, J. P., J. R. Koseff, and S. G. Monismith. 2007. Structure of mass and momentum fields over a model aggregation of benthic filter feeders. Biogeosciences **4**: 269–282. doi:10.5194/bg-4-269-2007.

Dade, W. B. 1993. Near-bed turbulence and hydrodynamic control of diffusional mass transfer at the sea floor. Limnol. Oceanogr. **38**: 52–69. doi:10.4319/lo.1993.38.1.0052.

Dame, R. F. 1999. Oyster reefs as components in estuarine nutrient cycling: Incidental or controlling? P. 267–280. *In* M. L. Luckenbach, R. Mann and J. A. Wesson [eds.], Oyster Reef Habitat Restoration: A Synopsis and Synthesis of Approaches. Virginia Institute of Marine Sciences.

Dame, R. F., J. D. Spurrier, and R. G. Zingmark. 1992. In situ metabolism of an oyster reef. J. Exp. Mar. Biol. Ecol. **164**: 147–159. doi:10.1016/0022-0981(92)90171-6.

Dame, R. F., T. Wolaver, and S. Libes. 1985. The summer uptake and release of nitrogen by an intertidal oyster reef. Neth. J. Sea Res. **19**: 265–268. doi:10.1016/0077-7579(85)90032-8.

Dedieu, K., C. Rabouille, G. Thouzeau, F. Jean, L. Chauvaud, J. Clavier, V. Mesnage, and S. Ogler. 2007. Benthic O2 distribution and dynamics in a Mediterranean lagoon (Thau, France): An in situ microelectrode study. Estuar. Coast. Shelf Sci. **72**: 393–405. doi:10.1016/j.ecss.2006.11.010.

Fréchette, M., C. A. Butman, and W. R. Geyer. 1989. The importance of boundary-layer flows in supplying phytoplankton to the benthic suspension feeder, *Mytilus edulis L*. Limnol. Oceanogr. **34**: 19–36. doi:10.4319/lo.1989.34.1.0019.

Genin, A., S. G. Monismith, M. A. Reidenbach, G. Yahel, and J. R. Koseff. 2009. Intense benthic grazing of phytoplankton in a coral reef. Limnol. Oceanogr. **54**: 938–951. doi:10.4319/lo.2009.54.3.0938.

Glud, R. N. 2008. Oxygen dynamics of marine sediments. Mar. Biol. Res. **4**: 243–289. doi:10.1080/17451000801888726.

Glud, R. N., O. Holby, F. Hoffmann, and D. E. Canfield. 1998. Benthic mineralization and exchange in Arctic sediments. Mar. Ecol. Prog. Ser. **173**: 237–251.

Gross, T. F., and A. R. Nowell. 1983. Mean flow and turbulence scaling in a tidal boundary layer. Cont. Shelf Res. **2**: 109–126. doi:10.1016/0278-4343(83)90011-0.

Hansen, J. C. R., and M. A. Reidenbach. 2012. Wave and tidally driven flows in eelgrass beds and their effect on sediment suspension. Mar. Ecol. Prog. Ser. **448**: 271–287. doi:10.3354/meps09225.

Hansen, J. C. R., and M. A. Reidenbach. 2013. Seasonal growth and senescence of a *Zostera marina* seagrass meadow alters wave-dominated flow and sediment suspension within a coastal bay. Estuar. Coasts. **36**: 1099–1114. doi:10.1007/s12237-013-9620-5.

Haven, D. S., and R. Morales-Alamo. 1966. Aspects of biodeposition by oysters and other invertebrate filter feeders. Limnol. Oceanogr. **11**: 487–498. doi:10.4319/lo.1966.11.4.0487.

Hume, A. C., P. Berg, and K. J. Mcglathery. 2011. Dissolved oxygen fluxes and ecosystem metabolism in an eelgrass (*Zostera marina*) meadow measured with the eddy correlation technique. Limnol. Oceanogr. **56**: 86–96. doi:10.4319/lo.2011.56.1.0086.

Jones, N. L., J. K. Thompson, K. R. Arrigo, and S. G. Monismith. 2009. Hydrodynamic control of phytoplankton loss to the benthos in an estuarine environment. Limnol. Oceanogr. **54**: 952–969. doi:10.4319/lo.2009.54.3.0952.

Lawson, S. E., P. L. Wiberg, K. J. McGlatherty, and D. C. Fugate. 2007. Wind-driven sediment suspension controls light availability in a shallow coastal lagoon. Estuar. Coasts. **30**: 102–112.

Lenihan, H. S. 1999. Physical-biological coupling on oyster reefs: How habitat structure influences individual performance. Ecol. Monogr. **69**: 251–275.

Lorke, A., L. Umlauf, T. Jonas, and A. Wüest. 2002. Dynamics of turbulence in low-speed oscillating bottom-boundary layers of stratified basins. Environ. Fluid Mech. **2**: 291–313. doi:10.1023/A:1020450729821.

Lu, Y., R. G. Lueck, and D. Huang. 2000. Turbulence characteristics in a tidal channel. J. Phys. Oceanogr. **30**: 855–867. doi:10.1175/1520-0485(2000)030<0855:TCIATC>2.0.CO;2.

MacMahan, J., A. Reniers, W. Ashley, and E. Thornton. 2012. Frequency–wavenumber velocity spectra, Taylor's hypothesis, and length scales in a natural gravel bed river. Water Resour. Res. **48**: W09548, doi:10.1029/2011WR011709.

McGlathery, K., I. C. Anderson, and A. C. Tyler. 2001. Magnitude and variability of benthic and pelagic metabolism in a temperate coastal lagoon. Mar. Ecol. Prog. Ser. **216**: 1–15. doi:10.3354/meps216001.

McGlathery, K., L. Reynolds, L. Cole, R. Orth, S. Marion, and A. Schwarzschild. 2012. Recovery trajectories during state change from bare sediment to eelgrass dominance. Mar. Ecol. Prog. Ser. **448**: 209–221. doi:10.3354/meps09574.

Mitchell, I. M. 2006. In situ biodeposition rates of Pacific oysters (*Crassostrea gigas*) on a marine farm in southern Tasmania (Australia). Aquaculture **257**: 194–203. doi:10.1016/j.aquaculture.2005.02.061.

Monismith, S. G., et al. 2010. Flow effects on benthic grazing on phytoplankton by a Caribbean reef. Limnol. Oceanogr. **55**: 1881–1892. doi:10.4319/lo.2010.55.5.1881.

Nelson, K. A, L. A. Leonard, M. H. Posey, T. D. Alphin, and M. A. Mallin. 2004. Using transplanted oyster (*Crassostrea virginica*) beds to improve water quality in small tidal creeks: A pilot study. J. Exp. Mar. Biol. Ecol. **298**: 347–368. doi:10.1016/S0022-0981(03)00367-8.

Newell, R. I. E. 1988. Ecological changes in Chesapeake Bay: Are they the result of overharvesting the American oyster, *Crassostrea virginica*? P. 536–546. *In* M. P. Lynch and E. C. Crome [eds.], Understanding the Estuary: Advances in Chesapeake Bay Research (Proceedings of a Conference, 29–31 March 1988, Baltimore, Maryland). CRC Publication 129. Chesapeake Bay Consortium.

Newell, R. I. E., and E. W. Koch. 2004. Modeling seagrass density and distribution in response to changes in turbidity stemming from bivalve filtration and seagrass sediment stabilization. Estuaries **27**: 793–806. doi:10.1007/BF02912041.

O'Connor, B. L., and M. Hondzo. 2008. Dissolved oxygen transfer to sediments by sweep and eject motions in aquatic environments. Limnol. Oceanogr. **53**: 566–578. doi:10.4319/lo.2008.53.2.0566.

O'Riordan, C. A., S. G. Monismith, and J. R. Koseff. 1993. A study of concentration boundary-layer formation over a bed of model bivalves. Limnol. Oceanogr. **38**: 1712–1729. doi:10.4319/lo.1993.38.8.1712.

Reidenbach, M. A., J. R. Koseff, and S. G. Monismith. 2007. Laboratory experiments of fine-scale mixing and mass transport within a coral canopy. Phys. Fluids. **19**: 075107, doi:10.1063/1.2752189.

Revsbech, N. P. 1989. An oxygen microsensor with a guard cathode. Limnol. Oceanogr. **34**: 474–478. doi:10.4319/lo.1989.34.2.0474.

Riisgård, H. U. 1988. Efficiency of particle retention and filtration rate in 6 species of Northeast American bivalves. Mar. Ecol. Prog. Ser. **45**: 217–223. doi:10.3354/meps045217.

Rippeth, T. P., E. Williams, and J. H. Simpson. 2002. Reynolds stress and turbulent energy production in a tidal channel. J. Phys. Oceanogr. **32**: 1242–1251. doi:10.1175/1520-0485(2002)032<1242:RSATEP>2.0.CO;2.

Roegner, G. C. 1998. Hydrodynamic control of the supply of suspended chlorophyll a to infaunal estuarine bivalves. Estuar. Coast. Shelf Sci. **47**: 369–384. doi:10.1006/ecss.1998.0351.

Røy, H., M. Hüttel, and B. B. Jørgensen. 2002. The role of small-scale sediment topography for oxygen flux across the diffusive boundary layer. Limnol. Oceanogr. **47**: 837–847. doi:10.4319/lo.2002.47.3.0837.

Schlichting, H., and K. Gersten. 2000. Boundary Layer Theory. 8th ed. Springer.

Shumway, S. E., and R. K. Koehn. 1982. Oxygen consumption in the American oyster *Crassostrea virginica*. Mar. Ecol. Prog. Ser. **9**: 59–68. doi:10.3354/meps009059.

Stacey, M. T., S. G. Monismith, and J. R. Burau. 1999. Measurements of Reynolds stress profiles in unstratified tidal flow. J. Geophys. Res. **104** (C5): 10933–10949. doi:10.1029/1998JC900095.

Steinberger, N., and M. Hondzo. 1999. Diffusional mass transfer at sediment-water interface. J. Environ. Eng. **125**: 192–200. doi:10.1061/(ASCE)0733-9372(1999)125:2(192).

Storlazzi, C., M. Field, and M. Bothner. 2011. The use (and misuse) of sediment traps in coral reef environments: Theory, observations, and suggested protocols. Coral Reefs **30**: 23–38. doi:10.1007/s00338-010-0705-3.

Whitman, E. R., and M. A. Reidenbach. 2012. Benthic flow environments affect recruitment of *Crassostrea virginica* larvae to an intertidal oyster reef. Mar. Ecol. Prog. Ser. **463**: 177–191. doi:10.3354/meps09882.

Widdows, J., M. D. Brinsley, P. N. Salkeld, and M. Elliott. 1998. Use of annular flumes to determine the influence of current velocity and biota on material flux at the sediment-water interface. Estuaries. **21**: 552–559. doi:10.2307/1353294.

Zhou, Y., H. Yang, T. Zhang, S. Liu, S. Zhang, Q. Liu, J. Xiang, and F. Zhang. 2006. Influence of filtering and biodeposition by the cultured scallop *Chlamys farreri* on benthic-pelagic coupling in a eutrophic bay in China. Mar. Ecol. Prog. Ser. **317**: 127–141. doi:10.3354/meps317127.

Received: 9 December 2012
Amended: 12 May 2013
Accepted: 12 September 2013